

Forced oscillations in applied respiratory physiology

Theoretical Principles

Andreas S. Lappas¹,
Anna Tzortzi^{1,2},
Panagiotis K. Behrakis^{1,2,3,4}

¹Smoking and Lung Cancer Research Centre, Hellenic Cancer Society, Greece

²Athens Medical Centre, Greece

³Harvard University, School of Public Health, USA

⁴Biomedical Research Foundation, Academy of Athens, Greece

Key-words:

- Forced oscillation technique
- Impulse oscillometry
- Respiratory resistance
- Respiratory reactance
- respiratory mechanics

Correspondence:

Andreas S. Lappas,
46 Mesogeion Ave., P.C. 11527, Athens, Greece
Tel.: 2107751641, 693074 2320, 2106470056
E-mail: andreaslappaswork@gmail.com.

SUMMARY. This is a literature review of the theoretical principles which frame the two widely used techniques of forced oscillations applied to the respiratory system, forced oscillation technique (FOT) and impulse oscillometry (IOS). The effect of forced oscillations on the respiratory system is investigated as a phenomenon of motion expressed as changes of pressure, volume, flow and acceleration in the classical mathematical approach to a linear system which, under the pressure of a stimulating force, is impelled into forced oscillation. The physiology of respiratory input impedance is presented as a parameter which describes the correlations between pressure, volume, flow, elastance, resistance and inertia of the respiratory system. The principles of basic practice for test completion are described, and the epidemiological factors which form the framework for the evaluation of the measurements, derived from research in healthy adults, are reviewed. *Pneumon 2013, 26(4):327-345.*

INTRODUCTION

The periodicity of the phenomenon of breathing is an integral part of respiratory mechanics, as it is linked with all fundamental parameters which define the functional level of the respiratory pump. One of the best theories highlighting the effect of breathing frequency on the configuration of alveolar ventilation is the linear approach to the volume-time relationship as formulated by Millic-Emili¹. According to this theory, in quiet breathing the alveolar carbon dioxide (CO₂) partial pressure is dependant on the physiological parameters of volume and time, according to the equation:

$$P_A\text{CO}_2 = \frac{(K \times V' \text{CO}_2)}{(V_T/T_i) \times (T_i/T_{\text{TOT}}) \times (1 - V_D/V_T)}^*$$

* where V_T = Tidal volume, T_{TOT} = period of the respiratory cycle, T_i = inspiratory time, T_e = expiratory time, f = breathing frequency, $P_A\text{CO}_2$ = alveolar carbon dioxide partial pressure, $V' \text{CO}_2$ = total CO₂ output, K = units constant, V_D = dead space

More recently reported approaches²⁻⁵, but also the previous study of the authors⁶ in which an improved harmonic vectorial approach to tidal breathing mechanics was formulated, document the way in which the fluctuation of breathing frequency significantly alters the energy demands of breathing. Data related to these modifications are expressed by the parameters forced oscillation technique (FOT) and impulse oscillometry (IOS), which constitute the most technically complete output of research on application of forced oscillations in clinical practice. FOT and IOS capture the effect of frequency on respiratory mechanics and thus add a new component to the study of respiratory function. A particular advantage of this method is the study and evaluation of quiet breathing, reflecting the everyday breathing activity of the subject.

Review of the theoretical basis of FOT and IOS is of importance, since a number of studies show how a better understanding of the theoretical principles upon which the application of forced oscillations is based has introduced new, important parameters into respiratory physiology. The use and usefulness of these parameters in clinical practice has been evaluated to a satisfactory extent, leading to conclusions indicative of the function of almost all the mechanical structures composing the respiratory system.

1. METHODOLOGY

1.1. The early application of forced oscillations in the human respiratory system

The first application of forced oscillations in humans, conducted by Du Bois and colleagues⁷ in 1956, consisted of the application of sinusoidal pressure waves of specific frequency [$f=(2-18)\text{Hz}$] to the surface of the body of a subject placed in a body box. The respiratory muscles of the subject were voluntarily relaxed at the end of a normal expiration, so that the respiratory system was balanced at the functional residual capacity (FRC) level. The apparatus used is depicted in Figure 1.

The pressure waves were produced by the reversible motion of a pump and the pressure changes around the chest of the subject led to a pressure difference between the airways opening and the outside of the chest (transthoracic pressure). The result was a passive imitation of normal breathing and flow production. The core significance of this apparatus is the application of harmonic forced oscillations on every anatomical

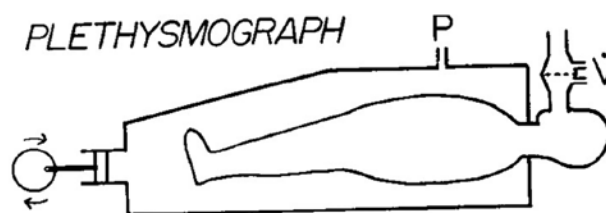


FIGURE 1. First application of forced oscillations. The subject lies in the supine position inside the body box. The pump is depicted moving reversibly, vertically to the long axis of the subject's body. The flowmeter (V') which is adjusted to the opening of the airways (the cavity of the mouth) is depicted. The pressure (P) and flow (V') signals are recorded at different points and thus transfer impedance values are measured. (Reproduced with the permission of DuBois *et al*⁷).

structure of the respiratory system, in order to study the changes on all the pressure and flow components, as described by the respiratory system equation of motion $P = E_{rs}V + R_{rs}V' + I_{rs}V''$ ⁸⁻¹⁰ at higher frequencies than those of quiet breathing.

The transfer impedance of the respiratory system was calculated as the ratio of the transthoracic pressure (recorded at the point corresponding to the symbol "P" of Figure 1) to the flow recorded by the flow-meter adjusted in the mouth cavity, at a range of frequencies of from 2 to 18 Hz.

This apparatus was subsequently replaced by that depicted in Figure 2. The sinusoidal pressure waves were applied at the airways opening, where the flow was also recorded, while the pressure difference created was now

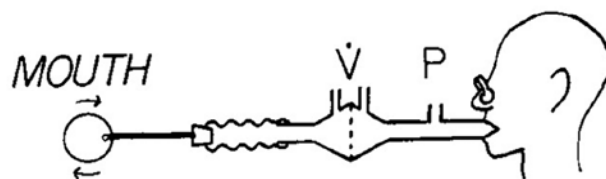


FIGURE 2. Advanced application of forced oscillations. A pump is depicted, moving reversibly, vertically to the sagittal axis of the head of the subject. The flow (V') and pressure (P) signals are both recorded at the opening of the airways (the cavity of the mouth) and thus input impedance values are measured. (Reproduced with the permission of DuBois *et al*⁷).

* P = minimum required pressure, necessary for the respiratory motion, V = volume, V' = flow, V'' = acceleration, E_{rs} = total respiratory system elastance, which is the reciprocal of the respiratory system compliance, R_{rs} = total respiratory system resistance, I_{rs} = coefficient of inertia of the respiratory system

the transrespiratory pressure (P_{rs}) (Figure 2).

The impedance was calculated as the ratio of P_{rs} to the flow and was called input impedance because the signals of both the flow and the pressure were recorded at the airways opening. Since that time, systems based on the second apparatus (Figure 2) have been used in the majority of oscillometry techniques, and input impedance values are measured.

1.2. Pressure and flow characteristics and multi-frequency input impedance definition

The graph of the change of P_{rs} versus time is depicted in Figure 3. P_{rs} is changed harmonically and the change can be imprinted mathematically in sinusoidal terms. Consequently, it is possible to define a period (T), a pressure change frequency ($f = 1/T$) and an amplitude of pressure (P_{max}). The mathematical formulation of a such change is: $P_{rs}(t) = P_{max} \sin(\omega t)$ (equation 1), where ω is angular frequency, $\omega = 2\pi f$, and f is the frequency of forced oscillations. Factor ωt is called *phase* of pressure change.

P_{rs} can be analyzed in components by applying the respiratory system equation of motion⁷⁻¹⁰:

$$P_{rs} = P_E + P_R + P_I = E_{rs}V + R_{rs}V' + I_{rs}V'' \quad (\text{equation 2})$$

and thus:

$$P_E = E_{rs}V, P_R = R_{rs}V' \text{ and } P_I = I_{rs}V''$$

The combination of equations 1 and 2 results in:

$$P_{rs}(t) = P_{max} \sin(\omega t) = E_{rs}V(t) + R_{rs}V'(t) + I_{rs}V''(t) \quad (\text{equation 3})$$

The solution of this differential equation according to time (t) is¹¹:

$$V(t) = -V_{max} \cos(\omega t) \quad (\text{equation 4})$$

$$V'(t) = V'_{max} \sin(\omega t) \quad (\text{equation 5})$$

$$V''(t) = V''_{max} \cos(\omega t) \quad (\text{equation 6})$$

where factors with status *max*, represent amplitudes (maximum absolute values) of the corresponding figures. The combination of equations 3, 4, 5 and 6 gives the time functions of each pressure component, in the following forms:

$$P_E = -E_{rs}V_{max} \cos(\omega t)$$

$$P_R = R_{rs}V'_{max} \sin(\omega t)$$

$$P_I = I_{rs}V''_{max} \cos(\omega t)$$

Based on the above equations, a vectorial approach to pressure components can be attempted. Each component

* P_{rs} = transrespiratory pressure, V = volume, V' = flow, V'' = acceleration, E_{rs} = total respiratory system elastance, which is the reciprocal of the respiratory system compliance, R_{rs} = total respiratory system resistance, I_{rs} = coefficient of inertia of the respiratory system, P_E = elastic recoil pressure, P_R =resistive pressure, P_I =inertial pressure

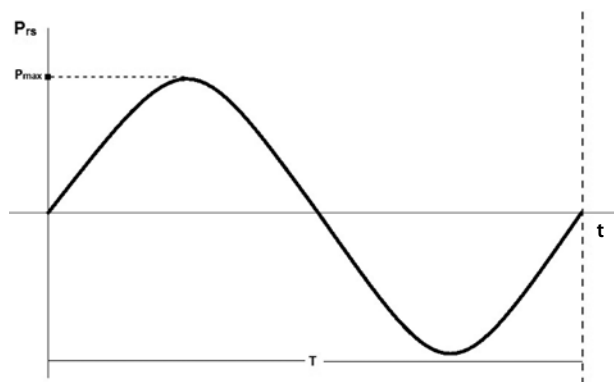


FIGURE 3. Graphical representation of change in transrespiratory pressure (P_{rs}) by time, which is a sinusoidal curve. P_{max} = pressure amplitude, T = pressure change period, where $T = 1/f$, and f = the pressure change frequency.

is considered as a vector with magnitude equal to the amplitude of the components and the direction imposed by the phase relationship of the components. The vectors are placed on the Cartesian level and the point (0.0) also is centred consider at their beginning. The vectors rotate with an angular velocity of $\omega = 2\pi f$ (rad/sec) around the point (0.0). This layout is depicted in Figure 4, where the

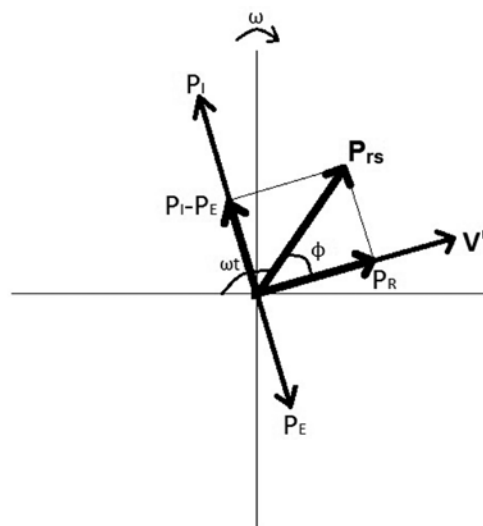


FIGURE 4. Representation of the vectors of elastic recoil pressure (P_E), resistive pressure (P_R), inertial pressure (P_I) and the resultant transrespiratory pressure (P_{rs}) vector, and the resultant of P_E and P_I ($P_I - P_E$) and the flow vector (V'). The vectors are rotating clockwise with angular velocity $\omega = 2\pi f$, where f is the frequency of the rotation. It can be observed that the phase difference (ϕ angle), which is formed by the vectors of P_{rs} and V' is positive, as it is pointing in the same direction as the sense of rotation of the vectors.

rotation has been conventionally chosen to be clockwise and the relationship of amplitude P_E and P_I arbitrary so that $P_E < P_I$. Angle ϕ , symbolizes the **phase difference** between the changes of resultant pressure (P_{rs}) and flow (V'), and is defined as the degree to which pressure **leads** flow¹².

Based on the above, it has been proven that flow changes harmonically with the same frequency (f) but P_{rs} and V' are out of phase, with a phase difference which equals ϕ . As shown in Figure 4, pressure leads flow, and thus ϕ is positive.

Here it must be pointed out that the sign of ϕ is not univocal and is defined by the magnitude of the vectors P_E and P_I and, therefore, the relationship of the amplitudes of P_E and P_I . In order to make the role of the relationship of P_E and P_I in forming ϕ comprehensible, we will choose the situation where the amplitude of P_E is greater than that of P_I . Now, as shown in Figure 5 the resultant pressure (P_{rs}) is on the fourth quadrant, angle ϕ becomes negative and the change of P_{rs} follows after flow change.

To generalize the above theory, we will study the changes of the x-axis projections of the vectors P_{rs} and V' . This change is expressed mathematically by the equations:

$$P_{rs}(t) = P_{max}\sin(\omega t) \quad (\text{equation 1})$$

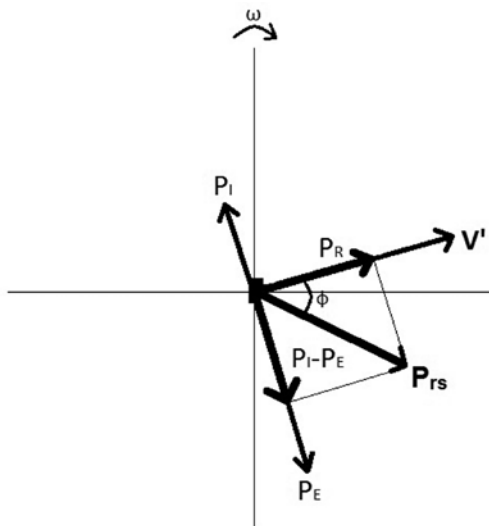


FIGURE 5. Representation of the vectors of elastic recoil pressure (P_E), resistive pressure (P_R), inertial pressure (P_I) and the resultant transrespiratory pressure (P_{rs}) vector, and the resultant of P_E and P_I ($P_I - P_E$) and flow vector (V'). The vectors are rotating clockwise with angular velocity $\omega = 2\pi f$, where f is the frequency of the rotation. It can be observed that the phase difference (ϕ angle), which is formed by the vectors of P_{rs} and V' is negative, as it is pointing in the opposite direction to the sense of the rotation of the vectors.

and $V'(t) = V'_{max}\sin(\omega t + \phi)$ (equation 7) where ϕ can have either a positive or a negative value, depending on P_E and P_I amplitude relationships. Equations 1 and 7 show also the change of transrespiratory pressure and flow versus time during harmonic forced oscillations and the relevant graphs are shown in Figures 6 and 7. In Figure 6, the pressure change leads flow change and the phase difference is positive, while in Figure 7, the pressure change follows after flow change and the phase difference is negative.

Impedance (Z) is the resultant of two components: (i) **Resistance (R)**, the values of which express the pressure and flow amplitudes relationship, and (ii) **Reactance**

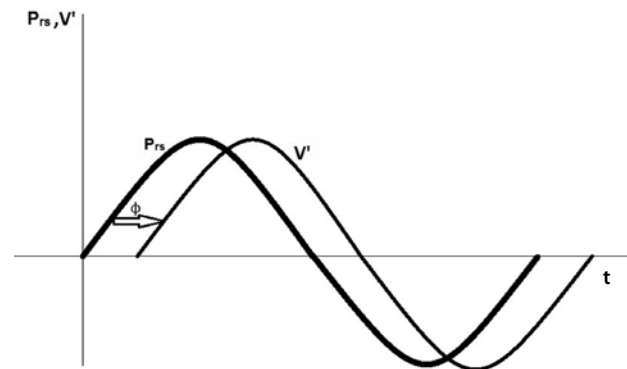


FIGURE 6. Depiction of changes of the X-axis projections of the vectors transrespiratory pressure (P_{rs}) and flow (V') by time. It can be observed that in this example pressure change leads to flow change, as described by the positive phase difference (ϕ angle) of the vectors P_{rs} and V' .

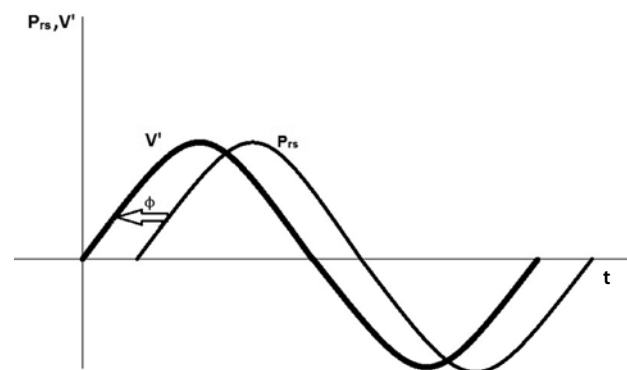


FIGURE 7. Depiction of changes of the X-axis projections of the vectors transrespiratory pressure (P_{rs}) and flow (V') by time. It can be observed that in this example pressure change follows after flow change, as described by the negative phase difference (ϕ angle) of the vectors P_{rs} and V' .

(**X**), which is the mathematical formulation of the time needed for the pressure change to cause flow change, in other words the phase difference as defined above. The values of **X** are thus formed by the phase relationship of pressure and flow. This mathematical description reflects the physiology of **X**. Reactance reflects the action of two components: the elastic properties of the anatomical structures of the respiratory system and the inertia of both the air column and the tissue (parenchymal or non parenchymal) elements of the system.

The effect of forced oscillations on the elastic element of the respiratory system causes firstly flow change which results in its distension and subsequent pressure change, in the form of elastic recoil pressure¹². Consequently, the phase difference is negative, since the pressure change comes after flow change. Conversely, in order to overcome the inertial forces, pressure change must be developed first, resulting in flow change^{6,12}. In this case the phase difference is positive, as the pressure change leads the flow change. Accordingly, in the case where the response of the elastic element in forced oscillations is dominant, which normally occurs in low frequency oscillations, the total pressure change follows the flow change, the phase difference is negative and therefore, the **X** values are also negative (Figures 5 and 7). The opposite occurs in a normal respiratory system in high frequency oscillations, where inertial forces are significantly higher due to the extremely high values of acceleration⁶ and the development of an adequate degree of pressure is needed to overcome them and create flow. Consequently pressure change leads flow change (Figures 4 and 6), the phase difference is positive and therefore, **X** values are also positive.

Based on these examples, it becomes clear that in a normal, "ideal" respiratory system the resistance values are not affected by the frequency of oscillation, in contrast with reactance values which depend on the frequency (**f**) of forced oscillations. This frequency defines ω directly (equation 1) and ϕ indirectly (equation 7).

Impedance, as the resultant of **R** and **X**, depends on frequency and therefore, different frequency values give different impedance values. Thus, a functional relationship is settled between impedance (**Z**) and frequency (**f**). The equation which describes this function is the following: $\mathbf{Z}(\mathbf{f}) = \mathbf{P}(\mathbf{f})/\mathbf{V}'(\mathbf{f})$, $\{0 \leq \mathbf{f} \leq \mathbf{f}_{\max}\}$ ¹³ and so, $\mathbf{Z}(\omega) = \mathbf{P}(\omega)/\mathbf{V}'(\omega)$, $\{0 \leq \omega \leq \omega_{\max}\}$, where $\omega = 2\pi f$ (equation 8).

1.3. Evolution and contemporary methodology of forced oscillation technique (FOT)

Understanding of the dependence of the mechanical

properties of the respiratory system on frequency led to the evolution of the method of FOT. Michaelson and colleagues¹⁴, based on the apparatus shown in Figure 2, in 1975 developed a computer driven loudspeaker which produced multifrequency pressure waves in the form of pseudorandom noise waveforms (PRN). These complex waves can be analysed in harmonics, based on the superposition principle, characterized by a specific, unique and separate frequency for each component. These waves were superimposed on the subject's tidal breathing, as software had been developed to discriminate between the components of tidal breathing (respiratory components) and the pressure and flow components created as a response to forced oscillations (oscillatory components). This technique, the FOT and is now widely used in lung function laboratories. Further development culminated in the precursor of the updated technique of oscillometry, introduced in 1976 by Landser and colleagues¹⁵, who, for the first time, applied pressure pulses on the respiratory tract of the subject. Since 1998, the pressure pulse technique has been perfected and has entered production under the name of impulse oscillometry (IOS)¹⁶.

The IOS technique is based on applying recurrent, alternating directed pressure "impulses" of 30-40 msec. duration, produced by an impulse generator^{12,13}. The pressure "impulses" are basically pressure changes (positive and negative), created by the reversible motion of the membrane of the generator's loudspeaker, and they are canalized to the respiratory tract of the subject during quiet breathing, forcing all the anatomic structures of the respiratory system into oscillatory motion. Forced oscillations are followed by flow and pressure changes ("impulse" components) the status of which is defined by the status of the pressure pulses and the elastance, resistance and inertia of the respiratory system. Input impedance of the respiratory system is calculated by the characters of pressure and flow, and expresses all mechanical properties of the system. Analysis of the physiology of impedance follows below.

Figure 8 shows the pressure and flow changes by time during IOS shown. These changes are not harmonic. The graphical representation of the time functions of "impulse" pressure and flow initially takes the shape of a triangle and subsequently approximately harmonic curves of infinitesimal amplitude in relation to the amplitude of the triangle. A safe approach of the equation of a such line is the following: $\mathbf{f}(\mathbf{t}) = 0.7 \text{UnitTriangle}[100/3(\mathbf{t}-1/50)] \sin(20\pi\mathbf{t}) - 0.1 \text{UnitTriangle}[200/3(\mathbf{t}-0.03-1/50)] \sin[50/3\pi(\mathbf{t}-0.04)]$ ¹⁸ (equation 9). *UnitTriangle* functions

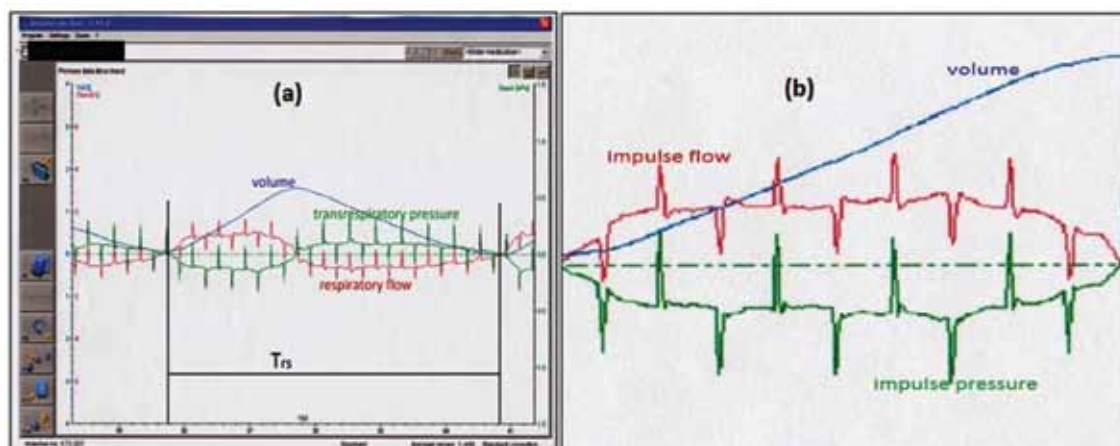


FIGURE 8. Depiction of tidal volume, flow and pressure changes by time, as recorded by the monitor of the computer during impulse oscillometry (IOS) on a healthy adult non-smoker. “Impulse” components (impulse pressure and impulse flow) are depicted magnified in Figure 6b. The green curve corresponds to the pressure change, the red curve to the flow change and the blue curve to the tidal volume. The period of the respiratory cycle is marked by the vertical black lines and described by the term T_{rs} .

describe a triangle-shaped waveform, and are multiplied by sinusoidal terms to describe more accurately the nature of the IOS generator products. Equation 9 is a far cry from the mathematical definition of a Dirac impulse, which is theoretically characterized by infinitesimal time duration and infinite amplitude. It is clear that during IOS such impulses are not produced, but in the framework of the mechanically feasible their characteristics make them almost factual, since they are produced in a 30-40msec period of time and have the appropriate amplitude for reliable impedance measurements^{13,18}.

The characteristic of equation 9 which indicates the peculiarity of the “impulses” produced by the IOS generator is the harmonic pattern which follows the initial triangular shape. By adding these, the equation tends to describe a *wave pulse* rather than an impulse. The mathematical description of a wave pulse is close to the actual nature of the activity and the products of the IOS “impulse” generator. The peculiarity of wave pulses lies in the lack of clear internal morphology of the wave, which is captured in the periodicity of the waveform (i.e., a short wave with no repeated oscillations – aperiodic waveform).

The mathematical definition of impedance measured by IOS is that of equation 8. In other words, about it refers to multi-frequency input impedance values, but there is a quality difference between the two definitions: equation 8, which derives from spectral analysis of each pressure and flow pulse of IOS is continuous in its domain, whereas the same function coming from spectral analysis of each pressure and flow wave of FOT is discontinuous. This

circumstance derives from the way the spectral analysis of pressure and flow waves is made. The core of the mathematical reasoning for this analysis is the transformation of the function of time describing each pressure and flow wave – $P(t)$ and $V'(t)$ -, to functions of frequency – $P(f)$ and $V'(f)$. This transformation can be made using an algorithm called fast Fourier transformation (FFT)¹⁹.

In the case of FOT, every multi-frequency pressure and flow wave is analyzed according to its components, based on the Fourier series inside FFT, and the components which result are integer multiples of the fundamental frequencies of the original periodical wave being analyzed¹⁹. Consequently, functions $P(f)$ and $V'(f)$ are discontinuous in their domain, $\{0 \leq f \leq f_{max}\}$, if this is considered as a subset of the real numbers. The function $Z(f) = P(f)/V'(f)$, $\{0 \leq f \leq f_{max}\}$ is therefore also discontinuous. Conversely, in the case of IOS, where pressure and flow pulses follow the standard of a wave pulse, the Fourier Integral is used in FFT, and this results in all functions being continuous in their domain and becoming real functions of a real variable¹⁹.

The clinical importance of this difference is still a controversial issue. At least theoretically, the continuous frequency spectrum of IOS could be an advantage in revealing underlying pathology of a respiratory system which presents non-homogeneity of its impedance characteristics¹³. On the other hand, the specific frequencies of FOT impart a better signal to noise ratio (SNR) and, at the same time, the resistance-frequency $[R(f)]$ and reactance-frequency $[X(f)]$ curve morphology, which to date is the most important evaluation element for respira-

tory function, proves to be identical for both methods¹⁷.

2. IMPEDANCE AS A PARAMETER OF RESPIRATORY PHYSIOLOGY

2.1. The concept of impedance

The use of electric models, analogues of the respiratory system, is a classic method of studying respiratory mechanics²⁰⁻²⁵. A simple such electrical circuit model (Figure 9) consists of the following elements: a capacitor, a resistor and an inductor (simple RLC circuit). The circuit derives energy from an alternating voltage source with specific electromotive force.

(i) **The Capacitor**, is an electric charge storage device and, therefore, an storage device of energy in the form of electric energy. When the capacitor is linked to an electromotive force the electric charge motion caused charges the capacitor, which in this state has dynamic electric energy storage. When the electromotive force is removed from the circuit, the charged capacitor will spontaneously start to discharge, diverting the electrical dynamic energy stored during charging to flow (electric current). This behaviour of the capacitor corresponds to the behaviour of the respiratory system in normal inspiratory and expiratory phases respectively. When inhaling (active process), elastic work is produced and thus elastic energy is stored to be consumed spontaneously while exhaling (a passive process, without additional energy contribution). This correlation is formulated mathematically as follows:

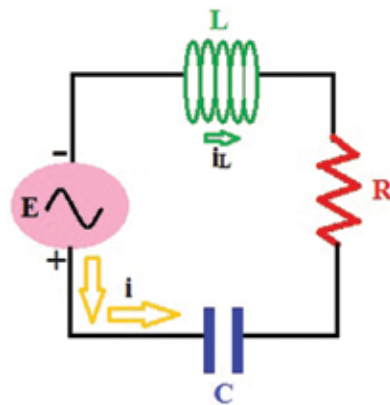


FIGURE 9. Depiction of a simple RLC circuit: I = electric current, C = capacitance, R = resistance, L = self-inductance, E = electromotive force of the source, i_L = field current created by the inductor.

(a) The electrical dynamic energy (U) that the capacitor stores while being charged is:

$$U = \frac{1}{2} Q^2/C^{26}$$

where Q is the electric charge and C the capacitance of the capacitor.

(b) The demanded work (W) for each respiration is:

$$W = \frac{1}{2} V_T^2/C_{rs}^{20}$$

where V_T is the tidal volume and C_{rs} , the respiratory system compliance. From this mathematical association the following rates result: the electrical charge (Q) of the capacitor in the electric circuit corresponds to volume, and the capacitance to respiratory system compliance (C_{rs}), or, in other words, the elastic properties of the system.

(ii) **The Resistor** is a device that prevents charge flow and converts the energy it carries to thermal energy. The resistance of the electric circuit can thus be paralleled to the total respiratory system resistance (R_{rs}), and the electric current (i) to flow (V').

(ii) **The Inductor** has the characteristic, unique capacity of resisting to the changes of electric current (i) in a circuit, causing inductive electromotive force with contrast armature to that of the source's electromotive force, and electric current (i_L) of the opposite direction to that going through its branch. It represents, in other words, the element of inertia inside the electrical circuit. Because of this capacity, it can be paralleled to inertial forces within the respiratory system ($I_{rs}V''$) as follows: (a) for inductive electromotive force: $E_L = -L (di/dt)^{26}$ (b) for the configuration of inertial forces within the respiratory system, the amount of pressure consumed: $P_I = I_{rs}V'' = I_{rs} (dV'/dt)$. Consequently, rate L (self-induction) corresponds to the inertial coefficient of the respiratory system (I_{rs}), and flow (V') to the electric current (i).

Figure 9 shows a simple RLC circuit model in which the energy the electromotive source produces is described by the equation $E = E_{max} \sin(\omega t)$, leading to the electric charge motion (i), described by the equation: $i = i_{max} \sin(\omega t + \phi)$. While the electric charge moves through the capacitor, resistor and inductor, part of the energy of the electromotive force of the source is spent:

$$E = V_C + V_R + V_L = 1/C \times Q + Ri + Li'^{*}$$

and so

$$E = 1/C \times Q + RQ' + LQ''^{26} \quad (\text{equation 10})$$

* V_C = voltage at the poles of the capacitor, V_R = voltage spent for the motion of the electric charge through the resistor, V_L = voltage created by the motion of the electric charge through the inductor, Q = total amount of moving charge, $Q' = dQ/dt = I$ = electric current, $Q'' = d^2Q/dt^2 = i'$ = electric charge acceleration, C = capacitance, R = resistance, L = inductance

The similarity of equation 10 to the respiratory system equation of motion ($P = 1/C_{rs} \times V + R_{rs} V' + I_{rs} V''$) verifies that through a linear approach with one degree of freedom, the respiratory system behaves like the electrical circuit of Figure 9^{7,20-25}.

Accordingly, the correlations of the above parameters can be extended to the respiratory input impedance definition, which will arise from resolution of this circuit. The resolution of this circuit is based on the transformation of time functions of the source's electromotive force and electric current into frequency functions and gives the following mathematical formulation of total impedance of the circuit in Cartesian complex form:

$$Z(\omega) = E_{\max}(\omega) / i_{\max}(\omega) = R + j(X_L - X_C) = R + j(\omega L - 1/\omega C)$$

where $\omega = 2\pi f$ ²⁶.

The element $X_C = 1/\omega C$ is called capacitive impedance and the element $X_L = \omega L$, inductive impedance. Factor j is the imaginary numbers coefficient, where $j^2 = -1$. The total impedance of the RLC circuit expresses the total barrier in the motion of the electric charge in the circuit and extends the meaning of resistance in alternating current circuits, where voltage (E) and current (i) are out of phase.

Exactly the same reasoning constitutes the mechanism by which the parameters of the respiratory system mechanics are evaluated by oscillometry. The time functions of pressure and flow $-P(t)$ and $V'(t)$ are transformed into frequency functions, with FFT.

The frequency functions that result are, qualitatively and quantitatively equivalent to those resulting from the resolution of the circuit RLC. Therefore, the mathematical expression of total respiratory input impedance (Z_{rs}), is as follows:

$$Z_{rs}(\omega) = P_{\max}(\omega) / V'_{\max}(\omega) = R_{rs} + jX_{rs} = R_{rs} + j(\omega I_{rs} - 1/\omega C_{rs})$$

where $\omega = 2\pi f$, $\{0 < f \leq f_{\max}\}$ (equation 11)

Thus, total impedance of the respiratory system expresses the total load, the "barrier", which is surmounted at every moment of respiratory motion.

In the circuit shown in Figure 9, the stimulator of oscillations is the source which "feeds" the circuit constantly with power in the form of voltage, resulting in the creation of a continuous flow of electric charge, compensating each time for the losses caused by resistance, self-induction and the charge of the capacitor. Thus, every single moment and for each value of the total charge of the circuit (Q), the equilibrium of the components of the circuit is given by the equation:

$$E = 1/C \times Q + RQ' + LQ''.$$

During FOT and IOS the stimulant is the applied pressure waves, or pulses (P_{appl}), produced by the generator. By applying P_{appl} , oscillatory components of flow and pressure are produced, surmounting the resistance, the elastic forces and the inertia of the respiratory system. Thus, every single moment, the equilibrium of the components of the respiratory system motion is described by the equation of motion:

$$P_{\text{appl}} = 1/C_{rs} \times V + R_{rs} V' + I_{rs} V''$$

2.2. Components of Impedance

Equation 10 can be analyzed with the following equations:

$$Z_{rs} = R_{rs} + jX_{rs} \quad (\text{equation 11}),$$

$$\text{and } Z_{rs} = R_{rs} + j(\omega I_{rs} - 1/\omega C_{rs})$$

where $\omega = 2\pi f$, $\{0 < f \leq f_{\max}\}$ ⁷ (equation 12)

a) Resistance (R_{rs})

The component of impedance which concerns resistance, includes^{7,12,13,27-47}: (i) Airways resistance (R_{aw}), where $R_{aw} = (P_{alv} - P_{ao}) / V'$; (ii) The tissue - parenchymal component of lung resistance (R_{tis}) (iii) Chest wall and diaphragm resistance (R_{cw}). Oscillometry can evaluate all these components of resistance of the respiratory system, with great sensitivity in imprinting their modifications. It does not reveal, however, equal specificity for each of these components, with the only exception the discrimination between central and peripheral resistance. High frequency resistance values (R_{rs} in 20 Hz) are formed mainly by central airways resistance, while low frequency resistance values are formed mainly by peripheral airways resistance (an interpretation of this phenomenon follows below). The R_{rs} of a healthy adult remains almost stable throughout the frequency range (when conventional oscillometry, with a frequency range of from 4 to 35 Hz, is applied) (Figure 10).

β) Reactance (X_{rs})

Reactance consists of^{7,12,13,27-47}: 1) a component which represents the energy contribution of the inertial forces (inertial component of X_{rs}), which is described by the term ωI_{rs} , in equation 12. Inertial forces are modulated by: (i) motion of the air-column in the central airways, and (ii) motion of the total tissue mass of the respiratory system (parenchymal or non parenchymal)^{6,7,21,38}. This component expresses the pressure-acceleration relationship, and its clinical value is still questioned^{13,35}. 2) A component which represents the elastic properties of the respiratory

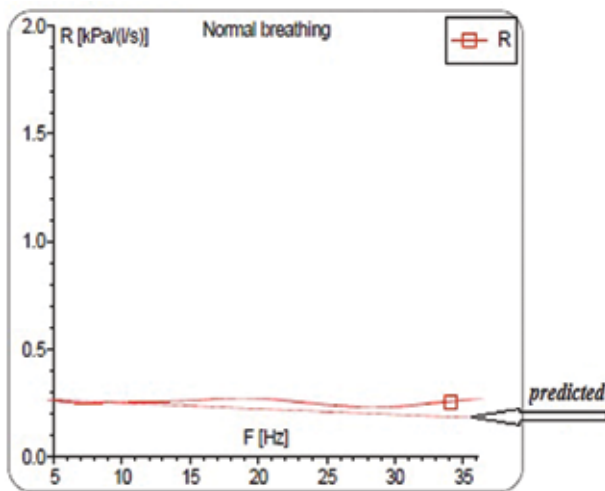


FIGURE 10. Impulse oscillometry (IOS): Depiction of the resistance (R_{rs}) – frequency (f) [$R_{rs}(f)$] curve of a healthy non-smoker of 23 years of age. [From the archives of the Centre for Smoking and Lung Cancer Research of the Hellenic Cancer Society, where the CareFusion (Master screen – IOS) machine is used]. It can be observed that the curve is almost rectilinear throughout the frequency spectrum (5-35 Hz).

system, and expresses the pressure-volume relationship (capacitive component of X_{rs}). This component is described by the term $1/\omega C_{rs}$ in equation 12⁷. C_{rs} refers to the total respiratory system compliance which contains lung and bronchial wall compliance, the compliance of the chest wall/abdominal compartment, thoracic gas compression and the upper airways compliance (mouth cavity, pharynx, etc.)^{7,38}.

It must be pointed out however, that the above approach, which derives from considering the respiratory system a linear system with properties analogous to those of a simple circuit RLC, is oversimplified. A more specific concept of the relationship between capacitive component of X_{rs} and compliance is described by the ratio $1/\omega C_{rs,dyn}$ ³⁸ where $C_{rs,dyn}$ is the total dynamic compliance of the respiratory system, consisting of the dynamic components referred to above. In a stricter approach, the concept of capacitive component of X_{rs} is not identical with that of compliance, but expresses the percentage of the total respiratory work which can be consumed for the production of elastic work and elastic energy storage^{13,38}. In order to avoid identification of this component with compliance, in contemporary bibliography equation 12 is slightly different from the original formulation by Du Bois and colleagues⁷, the new formulation of the equation being:

$$Z_{rs} = R_{rs} + j(\omega ln - 1/\omega Ca)$$

$$\text{with } \omega = 2\pi f, \{0 < f \leq f_{max}\}^{13,16} \text{ (equation 13)}$$

where the terms **Ca (capacitance)** and **ln (inertance)** express energy storage capacity³⁸.

During normal inspiration, elastic work is negative and reflects elastic energy storage⁶. Conversely, during normal quiet expiration (a passive process, with no additional energy contribution), elastic work is positive⁶ and mediates the return of the stored elastic energy to the respiratory system, causing motion and bringing the system back to its former state of equilibrium (FRC), surmounting resistance and inertial forces. **Capacitance** expresses the above sequence of elastic energy transport in the respiratory system. Inertial forces also contribute as an energy source throughout the respiratory cycle, as pointed out in a previous study of the authors⁶, in which it was demonstrated that in an “ideal” respiratory system, inertial forces are conservative, like elastic recoil forces. The pressure configured by inertial forces ($P_i = I_{rs} V''$), opposes the respiratory system motion at the beginning and up until the middle of inspiration or expiration (when it is nullified), resulting in the work of these forces being negative, unlike during the second half and up until the end of inspiration or expiration, when P_i tends to maintain respiratory system motion, resulting in inertial forces work being positive, and creating energy efficiency for the respiratory system. **Inertance**, expresses the energy transport that is mediated by inertial forces in the respiratory system.

At this point, in order to have a comprehensive view of the respiratory system behaviour under variable frequency circumstances, the resonant frequency (f_{res}) concept should be defined. In every forced oscillation system, the oscillation frequency is imposed by the stimulant. If the stimulant at any point is withdrawn the system will continue to oscillate with its inherent frequency, which is determined by the mechanical properties of the structures that constitute it, until attenuation forces bring a pause to the oscillation. This inherent frequency is the quality of an oscillating system and is not affected by external factors such as the frequency of the stimulant¹¹. f_{res} is the frequency of the stimulant which is equal (or almost equal in an attenuation system) to the inherent oscillation frequency of the system. In an RLC circuit, just as in oscillometry, when the frequency of the electromotive force or pressure waves respectively, is f_{res} , we can apply the format^{7,13,20}: $\omega_0 ln = 1/\omega_0 Ca$, $\omega_0 = 2\pi f_{res}$. Thus, f_{res} is the frequency at which, the inertial component is in equal quantity with the capacitive component, the value of X_{rs}

is zero ($X_{rs} = 0$) and the phase difference between pressure and flow is also zero ($\varphi = 0$).

As already mentioned, at frequencies lower than f_{res} , the capacitive component is dominant, while the inertial component is dominant at frequencies higher than f_{res} . Correspondingly, low frequency X_{rs} represents the periphery of the respiratory system where elastic energy storage capacity is greater, and the small peripheral airways where the flow is low and more linear, which results in small acceleration values, and depends on the supportive elastic tissue. High frequency X_{rs} expresses the behaviour of the larger, upper airways for the reverse reasons.

There is one interpretation of a technical nature of the specificity of the parameters of resistance (R_{rs}) and reactance (X_{rs}). It has been estimated that low frequency oscillations ($f < 20\text{Hz}$) are spread in a greater depth over generations of airways and reach the more peripheral parts of the bronchial tree, while the spread of high pressure frequency waves ($f > 20\text{Hz}$) is impeded in the middle sized airways and the waves never reach the periphery^{13,16}. The anatomical trace of frequency distribution and the precise point barrier of high frequency waves have never been clarified. It is estimated, based on Weibel's model, that this point is somewhere between the fifth and twelfth generations of airways¹⁶.

Figure 11 shows the reactance-frequency curve [$X_{rs}(f)$] of a healthy subject. The area under the curve, which is defined by the two coordinate axes and curve $X_{rs}(f)$, from its minimum rate (which is the point of intersection of the curve and axis y) to its rate in resonant frequency (which is the point of intersection of the curve and axis x), is called **reactance area (AX)**, giving^{12,13}:

$$AX = \int_5^{f_{res}} X_{rs} df$$

AX is a quantitative indicator of respiratory system reactance, at all frequencies between 5Hz and the resonant frequency. AX is an important magnitude as it evaluates three parameters: (i) the total X_{rs} of the respiratory system at frequencies lower than f_{res} , (ii) the resonant frequency (f_{res}), and (iii) the curvature of the function $X_{rs}(f)$. It has also been formulated that AX is a marker of airway closure, since such closure results in impending diffusion of pressure waves more peripherally in the bronchial tree, which is captured in the increase in the value of AX, expressing the increase of the "effective elastance" of the respiratory system³⁰. Figure 12 shows the graphical representation of all the frequency curves of resistance [$R_{rs}(f)$] and reactance [$X_{rs}(f)$] in a healthy subject.

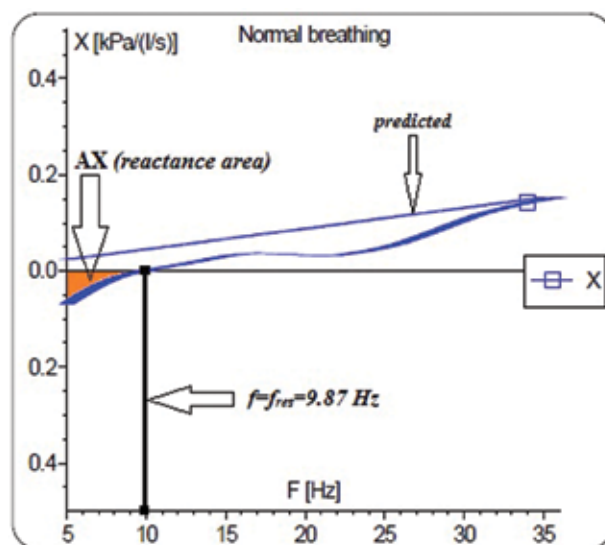


FIGURE 11. Impulse oscillometry (IOS): Depiction of the reactance (X_{rs}) – frequency (f) curve [$X_{rs}(f)$] of a healthy non-smoker of 23 years of age. [From the archives of the Centre for Smoking and Lung Cancer Research of the Hellenic Cancer Society, where the CareFusion (Master screen – IOS) machine is used]. The coloured area under the curve which is defined by the $X_{rs}(5)$ and $X_{rs}(f_{res}) = 0$ value, is called the reactance area (AX).

In conclusion, the parameters of the respiratory system mechanics that can be co-evaluated using oscillometry are the following: (i) R_c and R_p , corresponding to central and peripheral respiratory system resistance, consisting of the upper airways, peripheral airways, chest wall, diaphragm and tissue mass of the lung resistance³², (ii) $C_{extrathoracic}$: extrathoracic airways compliance, (iii) $C_{bronchial}$: bronchial tree compliance, (iv) C_{lung} : pulmonary compliance, (v) C_{cw} : chest wall and diaphragm compliance, (vi) I_{rs} : inertia of the air-column and the tissue mass (parenchymal or non parenchymal) of the respiratory system. Factors R_c and R_p are reflected in rates of the Ohmic component (R_{rs}), while factors $C_{extrathoracic}$, $C_{bronchial}$, C_{lung} , C_{cw} and I_{rs} are reflected in rates of reactance (X_{rs}). At this point, it must be emphasized that it is not feasible to record values of every one of the above components, but their values configure the rates of the parameters of impedance.

Figure 13 depicts a schematic rendering of an advanced electric model as proposed by Mead²¹ to describe all the parameters of the respiratory system mechanics listed above. This specific model is included unchanged in the IOS software to improve the specificity of the method towards each component of impedance. By using Mead's model, the IOS software can provide qualitative data for

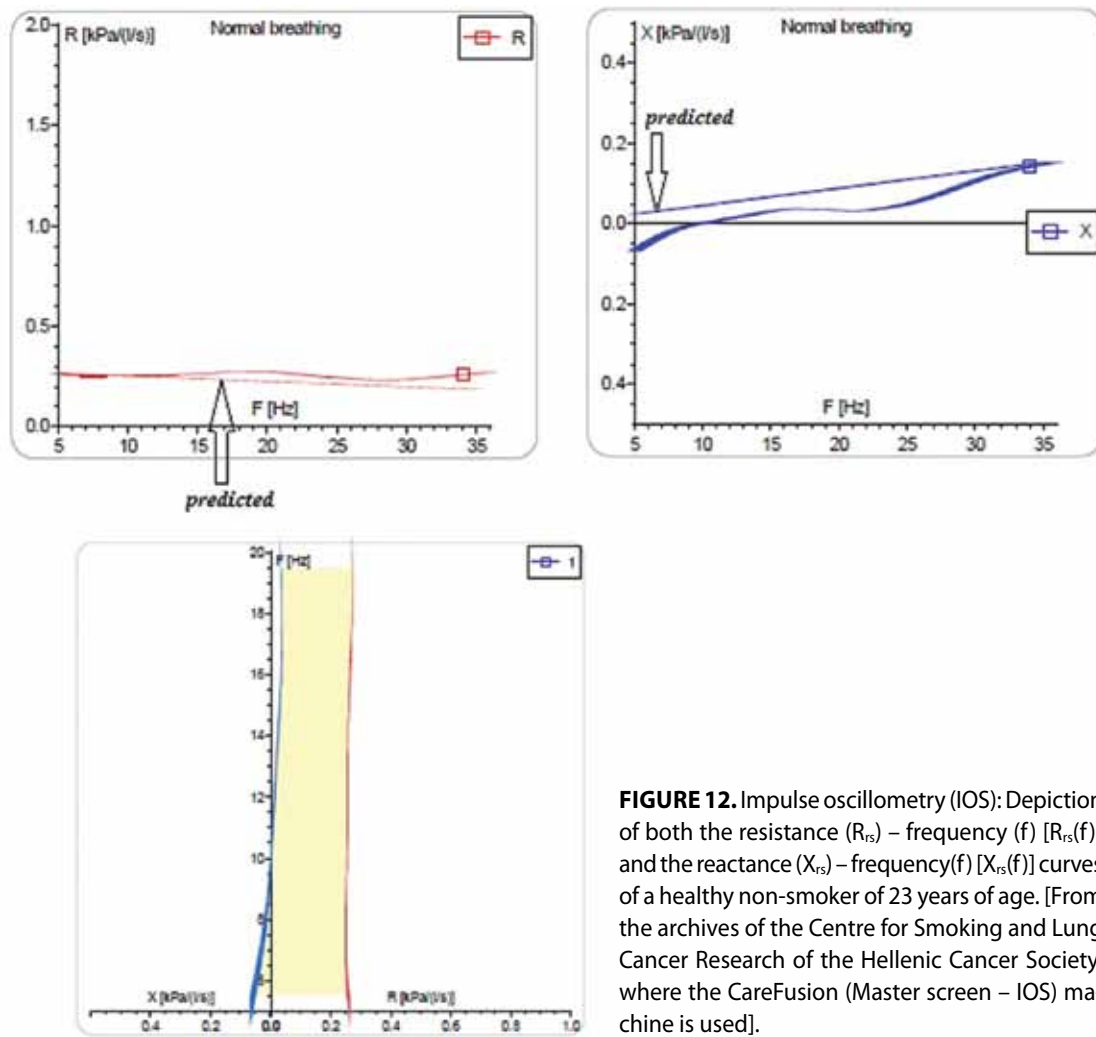


FIGURE 12. Impulse oscillometry (IOS): Depiction of both the resistance (R_{rs}) – frequency (f) [$R_{rs}(f)$] and the reactance (X_{rs}) – frequency (f) [$X_{rs}(f)$] curves of a healthy non-smoker of 23 years of age. [From the archives of the Centre for Smoking and Lung Cancer Research of the Hellenic Cancer Society, where the CareFusion (Master screen – IOS) machine is used].

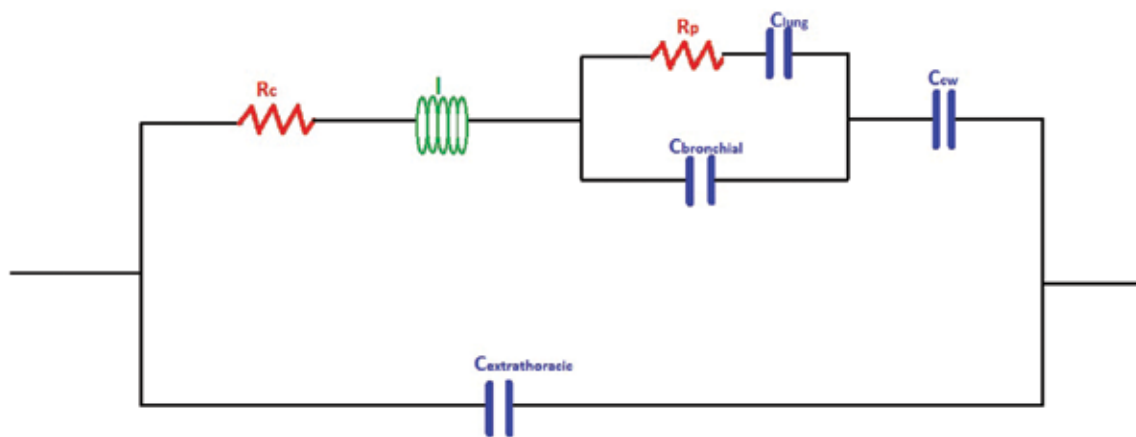


FIGURE 13. Depiction of a complex layout of capacitors, resistors and inductors, corresponding to the circuit introduced by J.Mead as an optimum electric analogue of the respiratory system. *Abbreviations:* R_c : central resistance, R_p : peripheral resistance, $C_{extrathoracic}$: extrathoracic airways compliance, C_{lung} : pulmonary compliance, C_{cw} : chest wall compliance, $C_{bronchial}$: bronchial tree compliance, I : inertia of the moving air-column and the tissue mass (parenchymal or not) of the respiratory system.

all of the above parameters of resistance, compliance, and inertia, which are shown in graphical presentation in Figure 14. Even this advanced model requires a simplified, one-dimensional approach to respiratory function and, therefore, deviations from the raw data of the parameters mentioned above are to be expected, especially for compliance, elastance and inertia values.

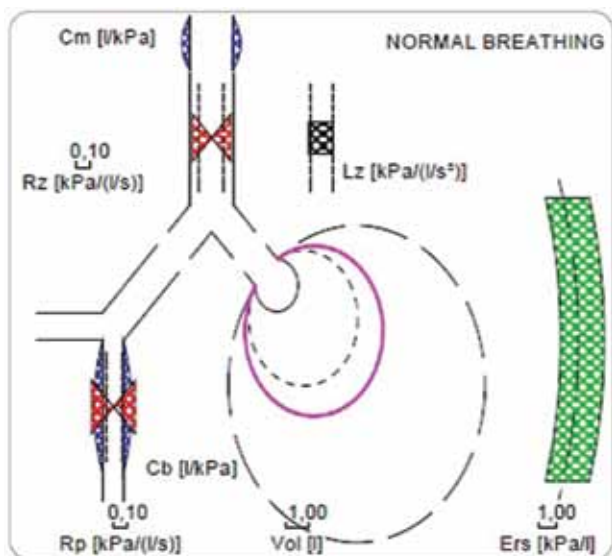


FIGURE 14. Graph of the qualitative data of compliance, elastance, resistance and inertia of the mechanical components of the respiratory system based on quantitative data of resistance and reactance, fitted to Mead's model. *Abbreviations:* C_m = extrathoracic airways compliance, R_z = upper airways resistance, L_z = respiratory system inertia, R_p = peripheral resistance, $E_{rs}=1/C_{rs}$ = total respiratory system elastance (reciprocal of the total respiratory system compliance).

3. SET UP, TECHNICAL CHARACTERISTICS AND PRACTICE PRINCIPLES FOR TEST COMPLETION

The FOT and IOS measuring heads are functionally similar. Both apparatuses have a forced oscillations generator with a loudspeaker to deliver the forced oscillatory signal, a low impedance pathway open to the atmosphere in order to achieve quiet breathing in the subject (to which usually a resistor is attached), a pneumotachograph, to which pressure and flow transducers are attached, and a mouthpiece which is attached at the end of the whole layout^{13,39}. Figure 15 shows a schematic rendering of the basic structures that compose the IOS measuring head.

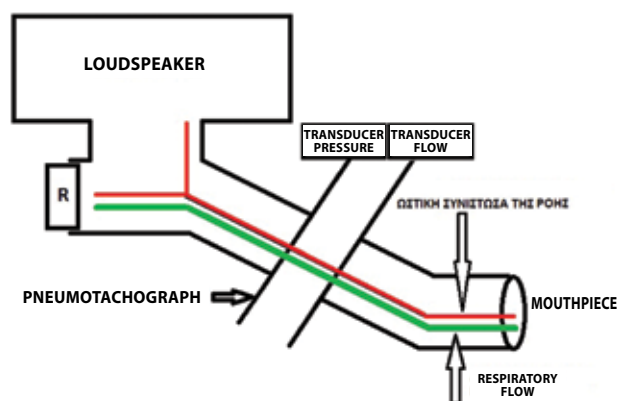


FIGURE 15. The basic constituent elements of the impulse oscillometry (IOS) measuring head: the loudspeaker (with a membrane which accelerates a volume displacement of 40mL in <40msec), connected to a Y-adaptor at one upper arm, an exit for respiratory flow with terminal resistor of resistance ~0.1 kPa/(L/s) at the second upper arm, and a lower arm adjusted to a Lilly-type pneumotachograph, which is connected with pressure and flow transducers. A mouthpiece is connected to the open side of the pneumotachograph. The green line corresponds to the respiratory flow, which is the first derivative of subject's tidal volume. The red line corresponds to the "impulse" flow, which is produced as a response to the pressure pulses. [Redrawn from Smith *et al.*¹³ Reproduced with the permission of the European Respiratory Society. *European Respiratory Society Monograph 2005; Eur Respir Mon 31 (Lung Function Testing) 72-105; DOI: 10.1183/1025448x.00031005*).

During the examination, the forced oscillations generator produces either pressure waves (FOT) or pressure pulses (IOS), which are channeled through the layout in Figure 15 to the respiratory tract of the subject. The pneumotachograph and the flow and pressure transducers receive complex pressure and flow signals which come from the breathing activity of the subject and from the superimposed forced oscillation signals (Figure 15). Those signals are separated, analyzed and digitalized by an analog to digital converter and are subjected to a standardization and sorting process which ensures the reliability of the measurements. As far as IOS is concerned, sampling intervals of 32 sampling points per impulse are used, corresponding to an optimized impulse rate of either 3 or 5 impulses per second, which results in the recording of 3 or 5 impedance spectra per second¹³. Recommendations have been formulated for optimizing the reliability of the measurements, which cover the apparatus, calibration and signal processing, including practice principles for examination completion³⁹. These recommendations refer

to FOT, but they are also applicable to IOS^{13,48}. Tables 1 and 2 outline the current recommendations for both techniques.

3.1. Artifacts

(i) Upper airway artifacts

Because of oscillatory motion of both the mouth cavity and, mostly, the extrathoracic airways⁴⁹, an amount of flow is produced which is included in the flow signal (V') and expresses the behaviour of these structures as an impedance (Z_{uaw}) - shunt in parallel to the true total impedance of the respiratory system (Z_{rs})⁴⁹⁻⁵³. As a result, a bias is established in measuring flow (V'), which leads to underestimation of total impedance (Z), as the denominator of the fraction systematically gets higher values: $Z(f) = P(f)/V'(f)$. This bias is of minimum influence

in the configuration of low frequency impedance values, but significantly interferes with the configuration of high frequency impedance values. This phenomenon affects the measurements of:

Resistance (R_{rs}), as an aberration from its normally almost stable value throughout the range of frequencies and establishment of a negative slope of the curve $R_{rs}(f)$ ^{16,39} which is called frequency dependence on resistance (fdr)

Reactance (X_{rs}), causing resonant frequency increase and shifting the $X_{rs}(f)$ curve towards more negative values^{16,39}.

These alterations constitute the characteristics of peripheral airways obstruction. Certain simple manipulations noted in Table 2 are thought to neutralize the upper airway artifact phenomenon effectively and provide safe data for clinical use^{13,16,39,48}.

TABLE 1. Recommendations for measurements made by forced oscillometric techniques concerning apparatus, calibration and signal processing^(13, 39, 48)

Apparatus	
Total impedance of the system (total load against spontaneous breathing)	<0.1 kPa/(L/s), below 5 Hz
Highest pressure developed in the system	≤0.5 kPa
Common mode rejection ratio (CMRR) of the pressure transducer	≥60 dB up to the highest frequency investigated
Linearity of the pressure transducer	Up to at least 0.5 kPa (within 2%)
Linearity of the flowmeter	Up to at least 1 L/s (within 2%)
Calibration*	
Reference impedance (Z_{rs}) for adult population	~1.5 kPa/(L/s)
Maximum error after proper calibration	10% or 0.01 kPa/(L/s)
Input signal characters	
Peak-to-peak amplitude of pressure composite signal**	0.1-0.3 kPa
Frequency range***	FOT: 4-30 Hz, in the case of multi-frequency waveform application the lowest possible frequency, in the case of a single-frequency sinusoidal wave application**** IOS: 5-35 Hz

FOT = forced oscillation technique, IOS = impulse oscillometry

*The magnitude of impedance should be comparable at all measured frequencies to that of the highest Z_{rs} encountered or expected in the measured subject population⁽³⁹⁾

**Peak-to-peak amplitude of a certain parameter is defined as the difference between its maximum positive (+A) and its maximum negative (-A) value, when a harmonic change by time is concerned [$A - (-A) = 2A$]. This magnitude is used especially to describe properties of electric signals, and is correlated with the electric energy that the signal is able to bear.

***In the cases that $R_{rs}(f)$ and $X_{rs}(f)$ curves must be evaluated, application of pseudorandom noise waveforms (FOT) or pressure pulses (IOS) is optimal. Single-frequency sinusoidal waves are preferred for monitoring the airway patency and bronchomotor tone, or when variability of impedance indices throughout the respiratory cycle (breath by breath analysis) is evaluated⁽³⁹⁾.

****Single-frequency FOT in 5Hz is usually applied in these cases.

TABLE 2. Forced oscillometry: Recommendations for examination completion^{13,39,48}

Position of the subject	Nose-clip is applied and measurements are performed in the sitting position. The subject's body must be aligned with the measuring head to ensure maintenance of a neutral relaxed head and neck posture, avoiding additional motions or body postures that might affect impedance values. The cheeks must be supported by the subject (in order minimize the upper airway artifact)*, whose teeth and lips must be firmly adapted to the mouthpiece. The subject's tongue must be beneath the mouthpiece in order to avoid obstruction.
Quiet breathing of the subject	The subject is instructed to breathe quietly at FRC level in order to achieve volume amplitude equal to the subject's tidal volume. Further instructions concerning depth and frequency of tidal breathing must be avoided. Volume and flow signals must be evaluated continuously by the technician and any aberration from the quiet breathing pattern leads to the rejection of the results and a new attempt.
Volume and flow history	Volume and flow should be monitored for ≥ 30 seconds. At least 3 minutes of quiet breathing should intervene between a previously performed forced manoeuvre and the next test. It is recommended that oscillometry be performed before any other lung function test requiring forced manoeuvres, due to changes of the bronchomotor tone caused by such tests.
Number of measurements	3-5 measurement, between which the subject should come off the mouthpiece. For repeatability evaluation, especially when bronchomotor tests are required, baseline measurements may be repeated 10–20 minutes later.
Display of the results	Mean \pm SD is considered the optimum mode of display of results display. CV% is recommended for repeatability evaluation, at every measured frequency. Graphics containing qualitative parameters (Figure 14), must always be followed by corresponding raw data.

*In the case of severe peripheral airways obstruction, cheek support by the operator is recommended

(ii) Artifacts imposed by the position of the tongue and the addition of an antibacterial filter

The increase of the anatomical dead space by about 60 mL¹⁶, which follows the use of an antibacterial filter, but also caused by obstruction of the mouthpiece by the tongue, adds an acquired impedance, in series with Z_{rs} , which leads to an increase of resistance, stable throughout the range of frequencies, depicted as central airways obstruction¹⁶. In contrast, the values and frequency curve of X_{rs} at frequencies lower than resonant frequency will scarcely be affected. A slight increase in the higher frequencies can be expected, both in values of X_{rs} and slope of $X_{rs}(f)$. To avoid these alterations, if the use of filter is essential the measurements must be corrected on the basis of the impedance values of the filter³⁹.

(iii) Artifacts imposed by mechanical load on the respiratory system during examination.

Tight belts and clothing increase peripheral reactance (R_p) and must be removed from the subject^{13,48}. In addition, for patients with severe peripheral airway obstruction, cheek support imposes a significant mechanical load on the chest wall, from the elevation of the arms,

which results in deterioration of the normal kinetics of quiet breathing and marked variability in the impedance parameters. For this reason, support of the cheeks by the operator is recommended for these patients⁴⁸.

4. EPIDEMIOLOGICAL FACTORS WHICH FORM THE FRAMEWORK FOR THE EVALUATION OF OSCILLOMETRIC INDICES

4.1. Reference values of oscillometric indices for healthy adults

All of the studies conducted with a view to developing prediction equations for the determination of reference values and predicted frequency curves of impedance components, were performed with FOT and used multiple linear regression models. In the classical study of L ands er and colleagues⁵⁴, prediction equations were produced by fitting a fourth grade polynomial function on the $R_{rs}(f)$ and $X_{rs}(f)$ curves of a healthy adult male population. Thus, the independent variable of this function was frequency (f) and the dependent variable was resistance (R_{rs}), or reactance (X_{rs}):

$$R_{rs} \text{ (or } X_{rs}) = a \cdot f^4 + b \cdot f^3 + c \cdot f^2 + d \cdot f + e$$

where **a, b, c, d, e**, are constants and appear as: **kH+W+mA**.

Factors H, W, A represent height, weight and age respectively, while *k, l, m* are real numbers (negative, positive or zero) and represent the effect of the above factors (H,W,A) on the power of the prediction equation. In all of the more recent studies⁵⁴⁻⁶⁰, the same mathematical model has been used, with the same or different demographic parameters, while both the measured and predicted values were given separately for the two sexes, since there are statistically significant differences in the rates between males and females, which is probably due to the difference in lung volume. In all the studies⁵⁴⁻⁶⁰ without exception, the most significant predictor of the mean values of R_{rs} and X_{rs} , in the frequency range 4-30Hz, was height, with age and body weight being factors that increase the power of the prediction equation, but that individually are significantly weaker predictors.

The distribution pattern for R_{rs} and X_{rs} values in the frequency spectra described above (Figure 12), is confirmed by all the studies⁵⁴⁻⁶⁰, in the frequency range 4-30Hz. The mean values of R_{rs} and X_{rs} show minimal variations between the earlier and the later studies⁵⁴⁻⁵⁹. These values are as follows: (i) *The mean value of R_{rs} in healthy adult males, in the frequency range 4-30 Hz, is equal to 0.25-0.26 kPa/(L/s) with a standard deviation (SD) of 0.05-0.07 kPa/(L/s).* (ii) *The mean value of R_{rs} in healthy adult females, in the frequency range 4-30Hz is equal to 0.30-0.34 kPa/(L/s), with SD 0.06-0.07kPa/(L/s).* In the recent study, however, of Brown and colleagues⁶⁰, also using FOT, significantly higher values were documented (Table 3). The particular features of this study were the large number of subjects, the recording of mean values of resistance and reactance on individual frequencies, and the high age range of the subjects (18-

92 years). In this study⁶⁰, increase in height was found to be correlated to decrease in R_{rs} and increase in X_{rs} , while increase in weight showed the opposite correlations.

It must be pointed out here that, at least according to current bibliographic information, there are no reports of data related to prediction equations for IOS indices. In the few studies that IOS data on healthy adults are reported⁶¹⁻⁶⁴, the $R_{rs}(f)$ and $X_{rs}(f)$ curves follow the pattern noted above (Figure 12), and the values of R_{rs} and X_{rs} (Table 4), are closer to those presented by Brown and colleagues⁶⁰. In the study of Crim and colleagues⁶¹, statistical analysis was used to assess the degree of agreement between the values of R_{rs} measured at 20 Hz (Table 4) with values predicted from the equations proposed by Pasker and colleagues⁵⁵ applied to a healthy non-smoking population. Almost 95% of the values fell within limits of agreement, although the prediction equations tended to underestimate the higher values of R_{rs} measured at 20 Hz.

The common denominator in the limitations of the evaluation of the results of the studies reported above is the absence of recording R_{rs} and X_{rs} values at individual frequencies in the FOT studies⁵⁴⁻⁵⁹, as only mean values in a frequency range are given, with the exception of the study of Brown and colleagues, and failure to separate the values according to sex in the IOS studies⁶¹⁻⁶⁴. This could partially explain the fact that in the latter study, the mean values of R_{rs} and X_{rs} are recorded as being significantly higher throughout the frequency range. It should be noted that R_{rs} values measured with the IOS technique, are slightly higher than those measured with FOT, as Hellinckx and colleagues¹⁷ demonstrated in a study on a healthy population and patients with various respiratory problems [asthma, chronic obstructive pulmonary disease

TABLE 3. Forced oscillation technique (FOT). Mean values of total respiratory system resistance (R_{rs}) and reactance (X_{rs}) corresponding to individual frequencies, for healthy adults, according to Brown *et al*⁶⁰.

Males					Females				
N	Age range (y)	f (Hz)	R_{rs} [kPa/(L/s)]	X_{rs} [kPa/(L/s)]	N	Age range (y)	F (Hz)	R_{rs} [kPa/(L/s)]	X_{rs} [kPa/(L/s)]
341	55 (17)	6	2.92 (2.83, 3.03)	-0.37 (-0.40, -0.34)	563	55 (17)	6	3.56 (3.49, 3.67)	-0.51 (-0.54, -0.49)
		11	2.92 (2.83, 3.00)	0.21 (0.17, 0.24)			11	3.46 (3.35, 3.53)	0.17 (0.14, 0.19)
		19	2.72 (2.64, 2.83)	1.18 (1.13, 1.24)			19	3.29 (3.22, 3.39)	1.29 (1.26, 1.33)

Data are shown as:

(i) $\bar{X}(SD)$, where \bar{X} = mean value of the corresponding parameter, and SD = standard deviation

(ii) $\bar{X}(\text{min, max})$, where min is the minimum and max the maximum value of the group

F = frequency, N = number of subjects (Reproduced with permission of Brown *et al*⁶⁰).

TABLE 4. Mean values of total respiratory system resistance (R_{rs}) and reactance (X_{rs}) from studies in which the impulse oscillometry (IOS) technique was applied in healthy adults⁶¹⁻⁶⁴.

Study		N	Age range (y)	R_{rs5} [kPa/(L/s)]	R_{rs20} [kPa/(L/s)]	$R_{rs5}-R_{rs20}$ [kPa/(L/s)]	X_{rs5} [kPa/(L/s)]	AX (kPa/L)	f_{res} (Hz)
Williamson et al ^{64*}	Healthy non smokers	45	26 (2)	0.37 (0.34, 0.43)	0.37 (0.33, 0.41)	0.01 (-0.01, 0.43)	-0.12 (-0.14, -0.1)		10.5 (6.9, 11.8)
Kohlauf et al ⁶¹	Healthy non smokers	55	37 (8)	0.30 (0.10)	0.25 (0.09)		-0.10 (0.06)		10.8 (3.3)
Crim et al ⁶²	Healthy non smokers	223	54.3 (9)	0.33 (0.10)	0.26 (0.07)	0.07 (0.05)	-0.10 (0.06)	0.38 (0.04)	12.4 (3.4)
	Healthy smokers	322	55.2 (9)	0.31 (0.10)	0.25 (0.07)	0.06 (0.05)	-0.09 (0.05)	0.34 (0.03)	12.1 (3.2)
Kanda et al ⁶³	Healthy non smokers	29	70 (1.3)	0.27 (0.02)	0.25 (0.02)	0.02 (0.01)	-0.10 (0.01)		15.7 (1.2)

*data represented as median (interquartile range)

The rest of the data are presented as: $\bar{X}(SD)$, where \bar{X} = mean value of the corresponding parameter and SD = standard deviation
N = number of subjects, AX = reactance area, f_{res} = resonant frequency.

(COPD), cystic fibrosis and other diseases]. The difference was more marked at low frequencies (especially at higher low frequency resistance values), with a mean value of 0.14 ± 0.09 kPa/(L/s) at 5 and 6 Hz, and decreased at higher frequencies. X_{rs} values presented no significant differences over the full frequency range. The authors reached the conclusion that the IOS technique overestimates low frequency resistance values.

A characteristic of almost all of the above studies^{54-62,64} was that the age range was 26-58 years and the common conclusion was that age is a weak predictor. However, aging of the respiratory system is linked to R_{rs} changes, which are related to respective changes in the flow-volume curve. The changes in both cases usually reflect a progressive increase in peripheral airways resistance, as expressed by slightly increased low frequency R_{rs} values and f_{res} increase⁶⁵, and decrease of airways resistance (R_{aw})⁶⁶⁻⁶⁸, mainly due to reduction of respiratory system compliance. The latter observation was confirmed in the study of Brown and colleagues⁶⁰, where lower age was connected with reduction in the X_{rs} mean value.

The age effect in the configuration of R_{rs} values was investigated by Guo and colleagues⁶⁸ in a study using FOT. Height was found to be the best predictor for R_{rs} and X_{rs} values in healthy non smokers with an average age of 81 years, while the contribution of age and body weight was either non-significant or negligible. The predicted as well as the measured R_{rs} mean values at the frequency range of 4-30 Hz tended to be lower than those observed in the

studies reported above in both sexes [measured values $R_{rs,mean\ 4-30}$: 0.22 ± 0.06 kPa(L/s) for males, and 0.26 ± 0.06 kPa(L/s) for females]. These results were attributed to airway dilatation because of the increase of FRC observed in aging, and to the decrease of the respiratory system compliance. This indicates that the above mechanism influences to a greater extent the configuration of R_{rs} values at those ages, and counterbalances the mild increase of peripheral resistance^{66,68}. The same conclusion can be derived from observing the resistance values in Table 4, where a descending progress of R_{rs5} and R_{rs20} values is detected in parallel with age increase. At the same time a clear increase in f_{res} values is observed, which is strongly related to small airways obstruction⁶⁵.

4.2. Variability of oscillometric parameters in healthy adults

In all of the studies reported above⁵⁴⁻⁶⁵, the short term variability of R_{rs} and X_{rs} , estimated by the coefficient of variation index (CV%) is recorded from 5 to 15%. These rates are comparable to those of body-plethysmographic parameters (sG_{aw})³⁹ and, often, higher than those of spirometric indices (FEV1). A common characteristic in all the studies is that the variability of X_{rs} is much higher than that of R_{rs} , due to both physiological and numerical properties. In addition, it has been demonstrated that inspiratory R_{rs} and X_{rs} variability is significantly lower than that of the expiratory parameters throughout the frequency range⁶⁹⁻⁷² and the use of the former is suggested

to ensure safer clinical decision-making⁴⁸. The variability of the expiratory parameters, however, has proved to be especially useful in the early diagnosis of expiratory flow limitation and evaluation of the progress of peripheral airways obstruction.

CONCLUSIONS

Despite apparent difficulties, the theoretical principles that provide the framework for oscillometric techniques are the product of long-term research in primary fields of respiratory physiology. This review provides an analytical approach to the basic mathematical principles which are classically used in respiratory mechanics and applied in the study of quiet breathing, through oscillometric techniques. It is clear from the current state of knowledge, that impedance indices, as evaluated by FOT and IOS, express different and perhaps finer parameters of respiratory physiology than the conventional lung function tests, such as spirometry and body-plethysmography. This can be attributed to the inherent capacity of the method to evaluate quiet breathing, which cannot be more completely investigated using any other currently applied lung function test. Given the practical convenience of the method and the fact that its results are not affected by respiratory system fatigue, both features being due to the minimal requirement of quiet breathing of the subject, oscillometric techniques and their clinical applications constitute a constantly developing area for research but also for use in clinical practice.

REFERENCES

- Milic-Emili J, Aubier M. Some recent advances in the study of the control of breathing in patients with Chronic Obstructive Lung Disease. *Anesth Analg* 1980; 59:865-873.
- Dosman J, Bode F, Urbanetti J, Antic R, Martin R, Macklem PT. Role of inertia in the measurement of dynamic compliance. *J Appl Physiol* 1975; 38:64-69.
- D'Angelo E, Rocca E, Milic-Emili J. A model analysis of the effects of different inspiratory flow patterns on inspiratory work during mechanical ventilation. *Eur Respir Mon* 1999; 12:279-295.
- Barnas GM, Mills PJ, Mackenzie CF et al. Dependencies of respiratory system resistance and elastance on amplitude and frequency in the normal range of breathing. *Am Rev Respir Dis* 1991;143:240-244.
- Barnas GM, Campbell DN, Mackenzie CF et al. Lung, chest-wall, and total respiratory system resistances and elastances in the normal range of breathing. *Am Rev Respir Dis* 1992; 145:110-113.
- Lappas A, Anagnostopoulos N, Behrakis PK. Harmonic vectorial concept of tidal breathing; special reference to inertia. In: Daifoti ZP, Dimopoulos AM, Kittas C, Koutsilieris M, Stefanadis C, Pantos K (editors), National and Kapodistrian University of Athens, Volume in honor of Professor Denis Cokkinos. JB Parisianos, 2012, pp 525-540.
- DuBois AB, Brody AW, Lewis DH, Burgess BF. Oscillation mechanics of lungs and chest in man. *J Appl Physiol* 1956; 8:587-594.
- Rohrer F. Der Stomungswiderstand in den menschlichen Atemwegen und der Einfluss der unregelmäßigen Verzweigung des Bronchialsystems auf den Atmungsverlauf in verschiedenen Lungenbezirken. *Arch Ges Physiol* 1915;162:225-229.
- Rohrer F. Der Zusammenhand der Atemorgan. *Arch Ges Physiol* 1916;165:419.
- Rohrer F, Nakasone K, Wirz K. *Physiologie der Atembewegung Handbuch der normalen und Pathologischen Physiologie. II*, pp. 70-127, Berlin:Springer, 1925.
- Halliday D, Resnick R. Forced oscillations and resonance. In: Walker J(editor), *Fundamentals of Physics*, Volume I, John Wiley and Sons, USA, 2002, pp. 373-375.
- Goldman M. Clinical Application of Forced Oscillation. *Pulm Pharmacol Ther* 2001; 14:341-350.
- Smith HS, Reinhold P, Goldman MD. Forced oscillation technique and impulse oscillometry. *Eur Resp Mon* 2005; 31:72-105.
- Michaelson E, Grassman E, Peters W. Pulmonary mechanics by spectral analysis of forced random noise. *J Clin Invest* 1975; 56:1210-1230.
- Landsér FJ, Nagels J, Demedts M, Billiet L, Van de Woestijne KP. A new method to determine frequency characteristics of the respiratory system. *J Appl Physiol* 1976; 41: 101-106.
- Goldman M, Saadeh C, Ross D. Clinical applications of forced oscillation to assess peripheral airway function. *Respir Physiol Neurobiol* 2005; 148:179-194.
- Hellinckx J, Cauberghs M, De Boeck K, Demedts M. Evaluation of impulse oscillation system: comparison with forced oscillation technique and body plethysmography. *Eur Resp J* 2001; 31:72-105.
- Ramos C, Nazeran H, Goldman M, Diong B. Circuit analysis justifies a reduced Mead's model of the human respiratory impedance for impulse oscillometry data. *IEEE Eng Med Biol Mag* 2010:548-552.
- Halliday D, Resnick R. Waves in elastic media. In: Walker J(editor), *Fundamentals of Physics*, Volume I, John Wiley and Sons, USA, 2002, pp.463-496.
- Mead I. Mechanical properties of the lungs. *Physiol Revs* 1961; 41:281-306.
- Mead J, Milic-Emili J. Theory and methodology in respiratory mechanics with glossary of symbols. In: Fenn WO, Rahn H (editors), *Handbook of physiology, Section 3, Respiration, Volume 1*. American Physiological Association, Washington DC, 1964 pp. 363-376.
- Woo T, Diong B, Mansfield L et al. A comparison of various respiratory system models based on parameter estimates from impulse oscillometry data. *IEEE Eng Med Biol Mag* 2004:3828-3831.
- Diong B, Rajagiri A, Goldman M, Nazeran H. The augmented RIC model of the human respiratory system. *Med Bio Eng Comput.* 2009; 47:395-404.

24. Goldman M, Nazeran H, Ramos C. et al. Electrical circuit models of the human respiratory system reflect small airway impairment measured by impulse oscillation (IOS). *IEEE Eng Med Biol Mag* 2010;2467-2472.
25. Meraz E, Nazeran H, Goldman M, Nava P, Diong B. Impulse oscillometric features of lung function: towards computer-aided classification of respiratory diseases in children. *IEEE Eng Med Biol Mag* 2008;2443-2446.
26. Halliday D, Resnick R. *Electromagnetic Oscillations, Alternating current*. In: Walker J(editor), *Fundamentals of Physics, Volume II*, John Wiley and Sons, USA, 2002, pp.387-429.
27. Delavault E, Sumon G, Georges R. Characterization and validation of forced input method for respiratory impedance measurement. *Resp Physiol* 1980; 40:119-136.
28. Frantz ID, Close RH. Alveolar pressure swings during high frequency ventilation in rabbits. *Pediatr Res* 1985; 19:653-658.
29. Peslin R, Fredberg JJ. Oscillation mechanics of the respiratory system. In: Macklem P, Mead J (editors), *Handbook of Physiology, Section 3: The respiratory system. Vol. III: Mechanics of breathing*. American Physiological Society, Washington DC, 1986, pp. 145-177.
30. Thorpe CW, Bates JH. Effect of stochastic heterogeneity on lung impedance during acute bronchoconstriction: a model analysis. *J Appl Physiol* 1997; 82:1616-1625.
31. Horowitz JG, Siegel SD, Primiano FP, Chester EH. Computation of respiratory impedance from forced sinusoidal oscillations during breathing. *Comput Biomed Res* 1983; 16:499-521.
32. Peslin R, Fredberg JJ. Oscillation mechanics of the respiratory system. In: AP Fishman(editor), *Handbook of physiology. Section 3: The respiratory system*. American Physiological Society, 1986. Bethesda, Maryland, USA. pp 145-77.
33. Dorkin HL, Lutchen KR, Jackson AC. Human respiratory input impedance from 4 to 200Hz: physiological and modeling considerations. *J Appl Physiol* 1989; 67:1973-1981.
34. Neild JE, Twort CHC, Chinn S, et al. The repeatability and validity of respiratory resistance measured by the forced oscillation technique. *Resp Med* 1989; 83:111-118.
35. Lutchen KR, Sullivan A, Arbogast FT, Celli BR, Jackson AC. Use of transfer impedance measurements for clinical assessment of lung mechanics. *Am Respir Crit Care Med* 1998; 157:435-446.
36. Navajas D, Farre R. Oscillation mechanics. *Eur Resp Mon* 1999; 12:112-140.
37. Johnson BD, Beck KC, Zeballos JR, Weisman IM. Advances in pulmonary laboratory testing. *Chest* 1999; 116:1377-1387.
38. MacLeod D, Birch M. Respiratory input impedance measurement: forced oscillation methods. *IEEE Med Biol Eng Comput* 2001; 39:505-516.
39. Oostveen E, MacLeod D, Lorino R et al. The forced oscillation technique in clinical practice: methodology, recommendations and future developments. *Eur Respir J* 2003; 22:1026-1041.
40. Johnson MK, Birch M, Carter R, Kinsella J, Stevenson RD. Use of reactance to estimate transpulmonary resistance. *Eur Respir J* 2005; 25:1061-1069.
41. La Prad AS, Lutchen R. Respiratory impedance measurements for assessment of lung mechanics: focus on asthma. *Respir Physiol Neurobiol* 2008; 163:64-73.
42. Bates JHT, Suki B. Assessment of peripheral lung mechanics. *Respir Physiol Neurobiol* 2008; 163:54-63.
43. Frey U. Forced oscillation technique in infants and young children. *Pediatr Respir Rev* 2005; 6:246-254.
44. Nielsen K. Forced oscillation technique. *Pediatr Respir Rev* 2006; 7S:58-510.
45. Stocks J. Introduction and overview of preschool lung function testing. *Pediatr Respir Rev* 2006; 7S:52-54.
46. Arets HGM, Cornelis K, van der Ent. Measurements of airway mechanics in spontaneously breathing young children. *Pediatr Respir Rev* 2004; 5:77-84.
47. Beydon N. Pulmonary function testing in young children. *Pediatr Respir Rev* 2009; 10:208-213.
48. Blonshine S, Goldman MD. Optimizing performance of respiratory airflow measurements. *Chest* 2008; 134:1304-1309.
49. Cauberghs M, Van de Woestijne KP. Effect of upper airway shunt and series properties on respiratory impedance measurements. *J Appl Physiol* 1989; 66:2274-2279.
50. Peslin R, Duvivier C, Gallina C, Cervantes P. Upper airway artefact in respiratory impedance measurements. *Am Rev Respir Dis* 1985; 132:712-714.
51. Marchal F, Haouzi P, Peslin R, Duvivier C, Gallina C. Mechanical Properties of the Upper Airway Wall in Children and Their Influence on Respiratory Impedance Measurements. *Pediatr Pulmonol* 1992;13:28-33.
52. Desager KN, Cauberghs M, Naudts J, Van de Woestijne KP. Influence of upper airway shunt on total respiratory impedance in infants. *J Appl Physiol* 1997; 87:902-909.
53. Peslin R, Duvivier C, Jardin P. Upper airway walls impedance measured with head plethysmograph. *J Appl Physiol* 1984; 57:596-600.
54. Lãndsér FJ, Clément J, Van de Woestijne KP. Normal values of total respiratory resistance and reactance determined by forced oscillations: influence of smoking. *Chest* 1982; 81:586-591.
55. Pasker HG, Mertens I, Clément J, Van de Woestijne KP. Normal values of total respiratory input resistance and reactance for adult men and women. *Eur Respir Rev* 1994; 4:134-137.
56. Clément J, Lãndsér FJ, van de Woestijne KP. Total resistance and reactance in patients with respiratory complaints with and without airways obstruction. *Chest* 1983; 83:215-220.
57. Gimeno F, van der Weele LT, Koëter GH, van Altena R. Forced oscillation technique. Reference values for total respiratory resistance obtained with the Siemens Siregnost FD5. *Ann Allergy* 1992; 68:155-158.
58. Pasker HG, Schepers R, Clément J, Van de Woestijne KP. Total respiratory impedance measured by means of the forced oscillation technique in subjects with and without respiratory complaints. *Eur Respir J* 1996; 9:131-139.
59. Govaerts E, Cauberghs M, Demedts M, Van de Woestijne KP. Head generator versus conventional technique in respiratory input impedance measurements. *Eur Respir Rev* 1994; 4: 143-9.
60. Brown NJ, Xuan W, Salome CM et al. Reference equations for respiratory system resistance and reactance in adults. *Respir Physiol Neurobiol* 2010; 172:162-168.

61. Crim C, Celli B, Edwards LD et al. Respiratory system impedance with impulse oscillometry in healthy and COPD subjects: ECLIPSE baseline results. *Respiratory Medicine* 2011; 105:1069-1078.
62. Kohlhauf M, Brand P, Scheuch H, Haussinger K, Heyder J. Impulse oscillometry in healthy nonsmokers and asymptomatic smokers: effects of bronchial challenge with metacholine. *J Aerosol Med* 2001; 14:1-12.
63. Kanda S, Fujimoto K, Komatsu Y, Yasuo M, Hanaoka M, Kubo K. Evaluation of Respiratory Impedance in Asthma and COPD by an Impulse Oscillation System. *Inter Med* 2010; 49:23-30.
64. Williamson PA, Clearie K, Menzies D, Vaidynathan S, Lipworth BJ. Assessment of small-airways disease using alveolar nitric oxide and impulse oscillometry in asthma and COPD. *Lung* 2011;189:121-129.
65. Janssens JP, Pache JC, Nicod LP. Physiological changes in respiratory function associated with ageing. *Eur Respir J* 1999; 13:197-205.
66. Butler J, Caro CG, Alcalá R, Dubois AB. Physiological factors affecting airway resistance in normal subjects and in patients with obstructive respiratory disease. *J Clin Invest* 1960; 39: 584-591.
67. Crapo RO, Morris AH, Clayton PD, Nixon CR. Lung volumes in healthy nonsmoking adults. *Bull Eur Physiopathol Respir* 1982; 18:419-425.
68. Guo YF, Herrmann F, Michel JP, Janssens PJ. Normal values for respiratory resistance using forced oscillation in subjects older than 65 years old. *Eur Respir J* 2005; 26:602-608.
69. Goldstein D, Mead J. Total respiratory impedance immediately after panting. *J Appl Physiol* 1980; 48:1024-1048.
70. Cauberghe M, van den Woestijne KP. Changes of respiratory input impedance during breathing in humans. *J Appl Physiol* 1992; 73:2355-2362.
71. Kubota M, Shirai G, Nakamori T, Kokubo K, Masuda N, Kobayashi H. Low frequency oscillometry parameters are less variable during inspiration than during expiration. *Respir Physiol Neurobiol* 2009; 166:73-79.
72. Ohishi J, Kurosawa H, Ogawa H, Irokawa T, Hida W, Kohzaki M. Application of impulse oscillometry for within-breath analysis in patients with chronic obstructive pulmonary disease: pilot study. *BMJ Open* 2011; 2:e000184.